Optics with an Atom Laser Beam

Immanuel Bloch, Michael Köhl, Markus Greiner, Theodor W. Hänsch, and Tilman Esslinger

Sektion Physik, Ludwig-Maximilians-Universität, Schellingstrasse 4/III, D-80799 Munich, Germany
and Max-Planck-Institut für Quantenoptik, D-85748 Garching, Germany
(Received 29 November 2000; published 2 July 2001)

We report on the atom optical manipulation of an atom laser beam. Reflection, focusing, and its storage in a resonator are demonstrated. Precise and versatile mechanical control over an atom laser beam propagating in an inhomogeneous magnetic field is achieved by optically inducing spin flips between atomic ground states with different magnetic moment. The magnetic force acting on the atoms can thereby be effectively switched on and off. The surface of the atom optical element is determined by the resonance condition for the spin flip in the inhomogeneous magnetic field. More than 98% of the incident atom laser beam is reflected specularly.

The realization of atom lasers [1] opens up new intriguing perspectives in coherent atom optics. These novel atom sources are based on Bose-Einstein condensates (BEC) [2] from which a coherent matter wave beam is extracted. The unique properties of atom lasers will make it possible to enter an experimental regime in atom optics that is not accessible for thermal atom sources. In light optics the availability of coherent sources has substantially increased the range of photonic applications. Similarly, it is expected, that coherent matter wave sources will have a profound impact on applications such as atom interferometry [3], atom holography [4], or the manipulation of atomic beams on a nanometer scale.

To fulfill these expectations it is crucial to invent atom optical elements that are adapted to the demands of the new highly coherent atom sources. For thermal atom sources a variety of atom optical elements have been investigated [5], which redirect, split, or shape atomic beams using position- or time-dependent potentials. To preserve the coherence properties of atom lasers a very high "surface quality" of atom optical elements is required. The de Broglie wavelength of an atom laser beam can be well below ten nanometers. The effective surface roughness of atom optical elements should therefore be even smaller.

The most simple approach to realize a coherent matter wave source is to suddenly release a Bose-Einstein condensate from the magnetic trap. The mechanical manipulation of released condensates has been demonstrated using optical standing wave fields [6,7], suitably shaped off-resonant laser fields [8], and pulsed magnetic fields [9]. Because of the sudden switch-off of the confining potential the energy of the repulsive interaction between the atoms is transformed into kinetic energy. The velocity distribution of the released atoms is therefore much broader than the Heisenberg limit associated with the spatial size of the trapped condensate. The velocity spread is drastically reduced for atom lasers employing continuous output coupling, where a Fourier limited output can be approached [10] and interaction effects are minimized. The resulting monoenergetic atom laser beam is not susceptible to dispersive effects in the manipulation of coherent matter waves [8], which are unwanted in most atom optical applications.

In this Letter we report on the atom optical manipulation of an atom laser beam. We have realized a versatile atom optical element and demonstrate reflection, splitting, and focusing of the atom laser beam, as well as its storage in a resonator. This is accomplished by optically inducing spin flips between atomic ground states of different magnetic moment, thereby switching the force on and off that the atom laser beam experiences in an inhomogeneous magnetic field. By a suitable choice of the frequencies and polarizations of the Raman laser fields, the coupling between two specific ground states can be induced. This avoids restrictions in the coupling strengths and state selectivity that would be encountered when using rf or microwave fields.

The atom laser output is extracted from a ^{87}Rb Bose-Einstein condensate using continuous output coupling [11]. A weak and monochromatic radio-frequency field transfers the magnetically trapped atoms, which are condensed in the $|F = 1, m_F = -1\rangle$ state, into the untrapped $|F = 1, m_F = 0\rangle$ state (F: total angular momentum, m_F: magnetic quantum number). Gravity accelerates the untrapped atoms downwards and a well-collimated atom laser beam is formed, while the magnetic trap is still on. After ballistically propagating over a few hundred micrometers the atoms enter the spin-flip region, where two focused laser beams induce a two photon hyperfine Raman transition and transfer a variable fraction of atoms into the state $|F = 2, m_F = 1\rangle$ with the magnetic moment $\frac{1}{2}\mu_B$ (μ_B: Bohr magneton).

The state $|F = 2, m_F = 1\rangle$ is low-field seeking and the atoms experience the potential of the magnetic trap. The gradient of our trap in the vertical direction exceeds the gravitational force by 1 order of magnitude. Therefore the atoms are slowed down until they reverse their direction of motion. Traveling upwards the atoms pass through the laser field for a second time where they are spin flipped into the original state $|F = 1, m_F = 0\rangle$ and continue their motion on a ballistic trajectory [see

Fig. 1(b)]. When the Raman lasers are switched off before the atoms cross the interaction region a second time, the atoms remain in the magnetically trapped state; see Figs. 1(a) and 4.

The frequencies of the two laser fields that induce the Raman transitions are adjusted to drive the single photon $5S_{1/2}$ to $5P_{1/2}$ transition off resonance [see Fig. 2(a)]. The polarizations of the laser beams are chosen such that the lower frequency field drives π transitions and the higher frequency field drives σ transitions. Here the quantization axis is chosen parallel to the local magnetic field vector, which is oriented vertically in the spin-flip region. For both laser fields the single photon detuning Δ is large compared to the single photon Rabi frequencies Ω_1 and Ω_2. Spontaneous scattering of photons is therefore suppressed and the coupling between the states $|F = 1, m_F = 0\rangle$ and $|F = 2, m_F = 1\rangle$ can be described by an effective two level system, with a coupling strength of $\overline{\Omega}_0 = -\frac{\Omega_1\Omega_2^*}{2\Delta}$ [12].

The resonance condition for the spin-flip transition is fulfilled if the frequency difference between the two Raman lasers is equal to the hyperfine plus Zeeman splitting of the two atomic states. Copropagating laser beams are used in the experiment so that the Raman transition is not sensitive to the Doppler effect. The resonance condition mentioned above is fulfilled on a shell of constant magnetic field. In other words, the effective surface of the mirror in the inhomogeneous trapping potential is determined by the frequency difference between the two Raman laser beams, which can be controlled with high accuracy. The spin flip therefore occurs in a region which is much better localized than the waist of the Raman laser

beams. The distance between the spin-flip region and the coils, which produce the dc-magnetic field, is a few centimeters. Therefore static corrugations of the mirror surface on a smaller spatial scale, e.g., in the nanometer range, are not expected. To minimize fluctuations in the magnetic trapping field a highly stable current supply ($\Delta I/I < 10^{-4}$) is used and the trapping region is placed in a magnetic shield enclosure. Fluctuations in magnetic field strength or Raman laser power can cause a jitter of the height of the mirror, which could reduce the coherence of the reflected beam. These fluctuations can be minimized so that the mirror preserves the coherence of the atom laser beam [13].

In the experiment Bose-Einstein condensates of typically 7×10^5 ^{87}Rb atoms are produced in a quadrupole and Ioffe configuration trap [14] by evaporative cooling. The laser light used to drive the two photon Raman transition is generated by two extended cavity diode lasers [15]. A phase-locked loop [16] is employed to stabilize the frequency difference between the two lasers to a frequency reference, which is tunable at around 6.8 GHz corresponding to the hyperfine splitting of the ^{87}Rb ground state. Each of the phase-locked lasers is amplified by injection locking another laser diode. The amplified laser beams pass through acousto-optic modulators used for switching them on and off. Then the two beams are overlapped with orthogonal polarizations and fed into a single mode optical fiber. The fiber filters the spatial mode and ensures that the laser beams are exactly copropagating. After the fiber the laser beams are directed into the vacuum chamber and propagate along the symmetry axis (y direction) of the elongated magnetic trapping potential, in which the cigar shaped condensate is stored. The focus of the overlapping laser beams is positioned 400 μm below the condensate at $z_0 = -400$ μm. The beam waists are $w_z = 27$ μm in the vertical and $w_x = 500$ μm in the horizontal direction.

We experimentally determined the reflectivity of the spin-flip mirror, with the Raman lasers detuned by 70 GHz
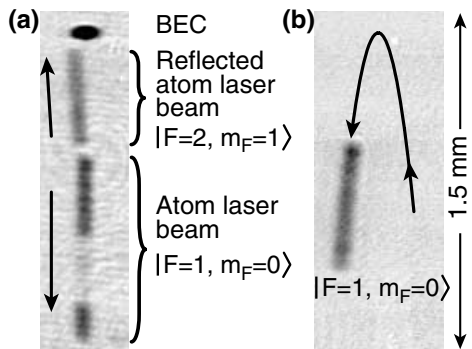

FIG. 1. Reflected atom laser beams for a single (a) and a double pass (b) through the Raman lasers. (a) The spin-flip mirror was switched on during a period of 2 ms. An adjustable fraction of the atom laser beam is spin flipped into the $|F = 2, m_F = 1\rangle$ state, reflected and moves upwards, as indicated by the arrow. The unaffected parts of the atom laser beam propagate downwards. (b) The spin-flip mirror was switched on for a sufficiently long time, so that all atoms that were spin flipped into the $|F = 2, m_F = 1\rangle$ state on their way downwards were spin flipped again back into the $|F = 1, m_F = 0\rangle$ state during their propagation upwards. The angle under which the beams are reflected is caused by a weak horizontal component of the magnetic field gradient at the position of the spin-flip mirror.
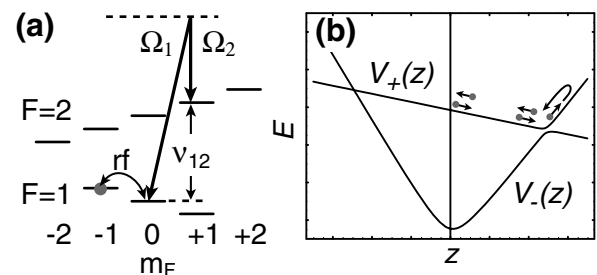

FIG. 2. (a) Level scheme of the $5S_{1/2}$ hyperfine ground state of ^{87}Rb in a magnetic field (not to scale). The condensate is produced in the $|F = 1, m_F = -1\rangle$ state and the atom laser is generated by coupling the condensate to the $|F = 1, m_F = 0\rangle$ state using an rf transition. The Raman lasers drive the two photon transition between the $|F = 1, m_F = 0\rangle$ and $|F = 2, m_F = 1\rangle$ states and are off resonance with the single photon excitation to the $5P_{1/2}$ state. (b) Adiabatic potentials $V_+(z)$ and $V_-(z)$ in the presence of the Raman lasers.

to the red of the D_1 line of ^{87}Rb and a magnetic field gradient of 200 G/cm [17]. An atom laser beam was extracted from the condensate for 4 ms. The Raman lasers were switched on 8.5 ms after the beginning of the output coupling for a duration of 2 ms. During this period of time a fraction of the atom laser beam was spin flipped into the $|F = 2, m_F = 1\rangle$ state and reflected. The magnetic trap was switched off 5 ms later and an absorption image was taken [see Fig. 1(a)]. The reflectivity of the mirror, i.e., the probability for spin flipping the atoms, was derived from the absorption images. The reduced optical density in that part of the atom laser beam which passed through the spin-flip region when the Raman lasers were switched on was compared to the optical density of the unperturbed atom laser beam. In addition, the optical density of the reflected, i.e., spin-flipped, part of the atom laser beam was measured. No loss of atoms was found in the reflection process. Figure 3 shows the mirror reflectivity vs the power of the Raman laser beams. For laser powers of 1.2 mW a peak reflectivity in excess of 98% was found.

The measured reflectivity can be described by adiabatic transitions according to a Landau-Zener model. The adiabatic potential curves for the atoms in a one-dimensional case are given by

$$V_{\pm}(z) = \frac{1}{2}[V_1(z) + V_0(z) \pm \sqrt{4\hbar^2 \bar{\Omega}^2(z) + \Delta_{12}^2(z)}],$$

(1)

where $V_1(z) = mgz + h\nu_{hf} + 1/2\mu_B \sqrt{B_0^2 + (B'z)^2}$ and $V_0(z) = mgz$ are the potentials for atoms in the $|F = 2, m_F = 1\rangle$ and $|F = 1, m_F = 0\rangle$ states, respectively (m: mass of ^{87}Rb, g: gravitational acceleration, h: Planck's constant). B_0 and B' denote bias field and radial gradient of the magnetic trap, which has an Ioffe-type magnetic field geometry [see Fig. 2(b)].

The frequency difference ν_{12} of the Raman lasers is detuned from the energy splitting of the trapped and untrapped atomic states by an amount $\Delta_{12}(z) = V_1(z) -$

$V_0(z) - \Delta_{AC}(z) - h\nu_{12}$, where Δ_{AC} is the residual difference in light shift induced by the Raman lasers that the atomic states experience. The spatial dependence of the Raman coupling is determined by the Gaussian laser focus $\bar{\Omega}(z) = \bar{\Omega}_0 e^{-2(z-z_0)^2/w_z^2}$.

The atoms pass through the interaction region with a velocity v which gives rise to nonadiabatic behavior. The probability for nonadiabatic passage is given by

$$p_{n.a.} = e^{-2\pi\Gamma},$$

(2)

with $\Gamma = \hbar \frac{\bar{\Omega}_0^2}{1/2\mu_B B' v}$. The efficiency of the adiabatic transition can thus be controlled by the atomic velocity v and $\bar{\Omega}$, which is proportional to the laser intensity. For the narrow longitudinal velocity spread of the atom laser beam the dependence on velocity of the Landau-Zener transition is negligible. In a numerical calculation we have verified that the finite interaction time of the atoms with the laser beam and its Gaussian shape results only in a slightly modified effective coupling strength and preserves the general form of the transition probability for our experimental parameters.

The optical access in the experiment allowed us to demonstrate reflection of the atom laser beam for various dropping heights of up to 0.8 mm. However, it is instructive to examine how the laser power required for adiabatic transitions scales with the dropping distance. From the criterion for adiabaticity $\frac{\bar{\Omega}_0 \tau}{2\Gamma} > 1$ [18], where $\tau = w_z/v$, we can estimate that the required Raman laser power $P = \sqrt{P_1 \times P_2}$ scales as $P \propto \sqrt{z_0}$, where z_0 is the dropping distance in the gravitational potential. Since for dropping heights of 0.5 mm only 1 mW of laser power is required, applying this scheme to much larger dropping heights is realistic. This is in contrast to atom optical mirrors using optically induced dipole potentials, where several watts of laser power are needed for reflection of atoms from the same dropping distance [8]. Furthermore, in the latter case the required laser power scales as $P \propto z_0$.

We have experimentally determined the specularity of the reflection process by comparing the transverse width of the atom laser beam before and after the reflection process. We have found that after a propagation time of 18 ms the width decreases by 25% ± 5%, which is in accordance with the weak curvature of the mirror in the axial direction. The transverse velocity spread of the atoms due to the reflection is well below 200 μm/s, which is the resolution limit in our experimental geometry. Limitations of the specularity are imposed by the profile of the Raman laser beams resulting in a phase modulation of the atom laser beam by the light shift potential V_{AC} in Eq. (1). From the spatial power spectrum of the laser profile we determine that at most 2% of the atoms are scattered out of the diffraction limit of the atomic beam. In comparison, evanescent wave mirrors or magnetic surface mirrors severely suffer from substantial diffuse reflection [19,20].

To demonstrate the versatility of the atom optical spin-flip element we have demonstrated the storage of the
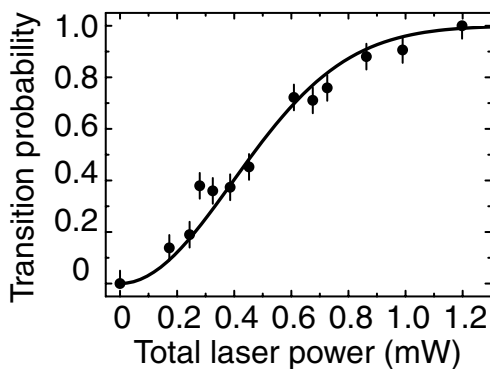

FIG. 3. Reflectivity of the spin-flip mirror. The curve shows the probability for an adiabatic transition as a function of the total intensity of the Raman laser beams. The full line is a fit to the data using the Landau-Zener model, as explained in the text. The scaling between the squared coupling strength $\bar{\Omega}_0^2$ and the laser intensity is taken as a free parameter.
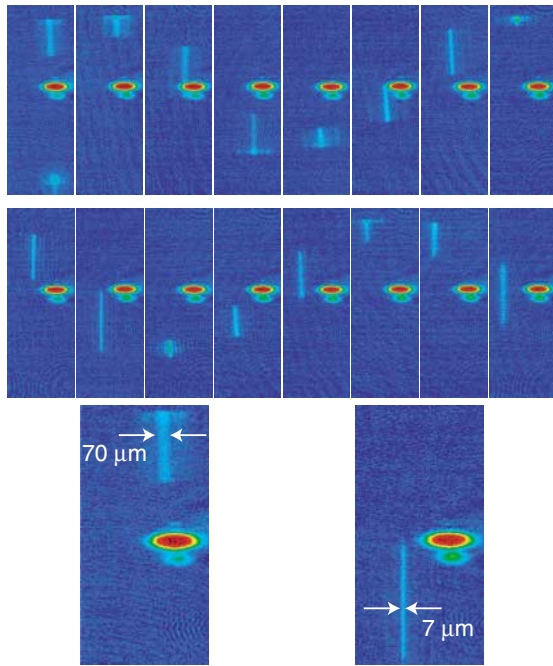
FIG. 4 (color).   Atom laser beam stored in a resonator formed by the magnetic trapping potential. The elliptical cloud in the center of each absorption image is the condensate. The stripe of varying width and length is the atom laser beam, which oscillates in the trap. Part of the atom laser beam which has not been recaptured can be seen in the first image of the upper row. Each image has a size of 2 mm $\times$ 0.7 mm. The two images in the bottom row show enlargements of the first image in the first row and the second image in the second row. The propagation time was increased by 2 ms for each image.

atom laser beam in the resonator formed by the magnetic trapping potential.   This was achieved by choosing a timing sequence for the Raman lasers such that the atoms in the atom laser beam were spin flipped only once. We could then observe the storage of the atom laser beam in the resonator formed by the magnetic trapping potential (Fig. 4). In this configuration we could monitor the atom laser beam for more than 35 oscillation periods. Because of the axial curvature of the magnetic trapping potential the atom laser beam was focused. The initial width of the atom laser beam is 70 μm, which is determined by the axial size of the BEC ground state in the magnetic trap. After a propagation period of 18 ms a width of the atom laser beam of only 7 μm, limited by the resolution of our imaging system, is measured.

Focusing of the atom laser beam is a central step towards an atom laser microscope [21]. To achieve a highly mono-energetic atom laser beam of short de Broglie wavelength our novel atom optical element could be used to accelerate the beam. It should then be possible to focus the beam to spot sizes much smaller than achievable in confocal light microscopy and comparable to high energy electron microscopy. An atomic fountain geometry as required for atomic clocks and atom interferometers [22] could be realized by shaping magnetic field gradients and cascading atom optical spin-flip elements.

In conclusion, we have demonstrated and quantitatively studied a versatile atom optical element which allows manipulation of an atom laser beam close to the diffraction limit in a free space environment. The experiments are crucial for future studies of fundamental properties of the atom laser and its applications.

---

 [1] M.-O. Mewes *et al.,* Phys. Rev. Lett. **78**, 582 (1997); B. P. Anderson and M. A. Kasevich, Science **282**, 1686 (1998); E. W. Hagley *et al.,* Science **283**, 1706 (1999); I. Bloch, T. W. Hänsch, and T. Esslinger, Phys. Rev. Lett. **82**, 3008 (1999).
 [2] M. H. Anderson *et al.,* Science **269**, 198 (1995); K. B. Davis *et al.*, Phys. Rev. Lett. **75**, 3969 (1995); C. C. Bradley *et al.,* Phys. Rev. Lett. **75**, 1687 (1995); **78**, 985 (1997).
 [3] *Atom Interferometry,* edited by P. Berman (Academic Press, New York, 1997).
 [4] M. Morinaga *et al.,* Phys. Rev. Lett. **77**, 802 (1996).
 [5] C. S. Adams, M. Sigel, and J. Mlynek, Phys. Rep. **240**, 143 (1994); B. Holst and W. Allison, Nature (London) **390**, 244 (1997); E. A. Hinds and I. G. Hughes, J. Phys. D **32**, R119 (1999).
 [6] M. Kozuma *et al.,* Phys. Rev. Lett. **82**, 871 (1999).
 [7] J. Stenger *et al.,* Phys. Rev. Lett. **82**, 4569 (1999).
 [8] K. Bongs *et al.,* Phys. Rev. Lett. **83**, 3577 (1999).
 [9] A. S. Arnold, C. MacCormick, and M. G. Boshier, in *Proceedings of the International Conference on Laser Spectroscopy XIV,* edited by R. Blatt, J. Eschner, D. Leibfried, and F. Schmidt-Kaler (World Scientific, Singapore, 1999); A. S. Arnold, Ph.D. thesis, University of Sussex, 1999.
[10] Y. B. Band, P. S. Julienne, and M. Trippenbach, Phys. Rev. A **59**, 3823 (1999).
[11] I. Bloch, T. W. Hänsch, and T. Esslinger, Phys. Rev. Lett. **82**, 3008 (1999); T. Esslinger, I. Bloch, and T. W. Hänsch, in *Proceedings of the International Conference on Laser Spectroscopy XIV* (Ref. [9]).
[12] B. W. Shore, *The Theory of Coherent Atomic Excitation* (Wiley-Interscience, New York, 1990).
[13] M. Köhl, T. W. Hänsch, and T. Esslinger, cond-mat/0104384.
[14] T. Esslinger, I. Bloch, and T. W. Hänsch, Phys. Rev. A **58**, R2664 (1998).
[15] L. Ricci *et al.,* Opt. Commun. **117**, 541 (1995).
[16] G. Santarelli, A. Clairon, S. N. Lea, and G. M. Tino, Opt. Commun. **104**, 339 (1994).
[17] When other values for the magnetic field gradient were chosen no fundamentally different behavior was found.
[18] J. R. Rubbmark, M. M. Kash, M. G. Littman, and D. Kleppner, Phys. Rev. A **23**, 3107 (1981); N. V. Vitanov and B. M. Garraway, Phys. Rev. A **53**, 4288 (1996).
[19] C. G. Aminoff *et al.,* Phys. Rev. Lett. **71**, 3083 (1993).
[20] E. A. Hinds and I. G. Hughes, J. Phys. D **32**, R119 (1999).
[21] V. I. Balykin and V. S. Letokhov, Opt. Commun. **64**, 151 (1987); R. B. Doak *et al.,* Phys. Rev. Lett. **83**, 4229 (1999).
[22] M. Kasevich, E. Riis, S. Chu, and R. deVoe, Phys. Rev. Lett. **63**, 612 (1989).